# Temperature dependence of the phonon and roton excitations in liquid $^4$He

W. G. Stirling
*Department of Physics, School of Physical Science and Engineering, University of Keele, Keele ST5 5BG, United Kingdom and Science and Engineering Research Council, Daresbury Laboratory, Warrington WA4 4AD, United Kingdom*

H. R. Glyde
*Department of Physics, University of Delaware, Newark, Delaware 19716*
(Received 28 August 1989)

We report high-precision neutron scattering measurements of the temperature dependence of the phonon and roton excitations in liquid $^4$He at saturated vapor pressure in both the superfluid and normal-fluid phases. Two wave vectors were examined in detail: $Q=0.4$ Å$^{-1}$ in the phonon region and $Q=1.925$ Å$^{-1}$ at the roton minimum. The goal is to understand excitations in Bose liquids by determining the dynamic structure factor $S(Q,\omega)$ accurately in both phases. At $Q=0.4$ Å$^{-1}$ the sharp peak in $S(Q,\omega)$ broadens with temperature $T$, but remains sharp and well defined in the normal phase ($T>T_\lambda$) up to $T\approx 3$ K. The rate of increase of the width of $S(Q,\omega)$ shows a break at $T_\lambda$, but otherwise $S(Q,\omega)$ is similar in the two phases and a transition could not be identified through $S(Q,\omega)$. In contrast at $Q=1.925$ Å$^{-1}$, the sharp component of $S(Q,\omega)$ disappears at $T_\lambda$ and $S(Q,\omega)$ is very different above and below $T_\lambda$. This behavior is documented and values of the frequencies and linewidths at several temperatures are reported.

## I. INTRODUCTION

Liquid $^4$He is the most readily accessible Bose quantum liquid in nature. It exhibits both a superfluid (Bose broken symmetry) and a normal state. Neutron inelastic scattering studies have provided detailed information[1] on the dynamical response of this fundamental Bose liquid. Nevertheless, the character and interpretation of the excitations observed in both the superfluid and normal phases, and especially the relation between the excitations in the two phases, is not clear.[1] In this paper we present high-precision measurements of the scattered intensity at wave vectors $Q=0.4$ Å$^{-1}$ and $Q=1.935$ Å$^{-1}$ over a wide temperature range in both the superfluid and normal phases. $Q=0.4$ Å$^{-1}$ and $Q=1.935$ Å$^{-1}$ lie in the "phonon" and "roton" regions, respectively, of the single excitation dispersion curve of the superfluid phase. The aim is to display the difference in the dynamical structure factor $S(Q,\omega)$ in the two phases, in an attempt to further understand the nature of the excitations.

In the superfluid phase (temperature $T<T_\lambda=2.17$ K at saturated vapor pressure (SVP), $S(Q,\omega)$ contains a single sharp peak superimposed on a broad background.[1] The sharp peak may be interpreted as the collective phonon-roton excitation in the fluid density proposed by Landau[2] and evaluated by Feynman[3] and others.[4] Within the Green's function[1,5–10] or dielectric formulation[11–17] of Bose fluids, the sharp peak may also be interpreted as excitation by the neutron of a single quasiparticle, a single, dressed particle[10] having momentum $p=\hbar Q$. The broad background may be interpreted as multiphonon or multiquasiparticle excitation.

Indeed, the dielectric theory shows that $S(Q,\omega)$ in the superfluid phase can be represented as the sum of a "singular" and a "regular" part. The singular part is defined as that part which is proportional to the single-particle Green's function $G_1(Q,\omega)$. In this way, the single-particle excitations can be observed in $S(Q,\omega)$. The appearance of $G_1(Q,\omega)$ in $S(Q,\omega)$ is due to a finite condensate fraction $n_0$. As $Q\to 0$, the poles of $S(Q,\omega)$ and $G_1(Q,\omega)$ coincide.[7] In the normal phase only the regular part survives in $S(Q,\omega)$ and single quasiparticle excitations cannot be observed via $S(Q,\omega)$. A central motivation here is therefore to explore possible differences in $S(Q,\omega)$ in the superfluid and normal phases. This is particularly interesting at lower $Q$ where the dielectric theory should be most applicable[7,17] and where recent, precise data are not available.

As temperature is increased in the superfluid phase, the sharp peak broadens.[1] This broadening may be well described[18] by quasiparticle-quasiparticle scattering, as proposed initially by Landau and Khalatnikov,[19] at least at low temperature. Precise data[20,21] at larger wave vectors ($Q\gtrsim 1$ Å$^{-1}$) suggest that the sharp peak disappears entirely from $S(Q,\omega)$ when $T$ is increased to $T_\lambda$, leaving only a broad $S(Q,\omega)$ in the normal phase. This is particularly clear in the data in the "maxon" region of the phonon-roton dispersion curve ($Q=1.1$ Å$^{-1}$).[20,22] This disappearance, or abrupt change in $S(Q,\omega)$, at $T_\lambda$ suggests that the sharp component in $S(Q,\omega)$ is a property of the superfluid phase. In the normal phase, $S(Q,\omega)$ is a broad function of $\omega$ and largely independent of temperature. As noted, in the dielectric theory, quasiparticle excitation can no longer be observed in $S(Q,\omega)$ in the normal phase where $n_0=0$.

On the basis of data at SVP for $Q\gtrsim 0.8$ Å$^{-1}$, Woods and Svensson[20] proposed that $S(Q,\omega)$ could be decomposed into two parts, a superfluid component $S_S(Q,\omega)$ and a normal component $S_N(Q,\omega)$. In the superfluid phase, each component was weighted by the respective

 

superfluid and normal densities $\rho_S(T)$ and $\rho_N(T)$ in the form,

$$S(Q,\omega)=[\rho_S(T)/\rho]S_S(Q,\omega)+[\rho_N(T)/\rho]S_N(Q,\omega) .$$

Recently, Talbot *et al.*[22] made precise measurements of the temperature dependence of $S(Q,\omega)$ over a wide range of $\omega$ in liquid $^4$He under 20 bars pressure. Two wave vectors were studied, $Q=1.13$ and 2.03 Å$^{-1}$, which correspond to the maxon and roton regions of the phonon-roton dispersion curve, respectively. As at SVP, the sharp peak in $S(Q,\omega)$ either vanished or changed abruptly as $T$ was increased through $T_\lambda$. However, Talbot *et al.*[22] found that the Woods-Svensson decomposition, with components proportional to $\rho_S(T)$ and $\rho_N(T)$, did not describe the data accurately enough to have fundamental meaning. The important observation by Woods and Svensson[20] that $S(Q,\omega)$ changed abruptly at $T_\lambda$ for $Q \gtrsim 1$ Å$^{-1}$ was confirmed.

As noted, the temperature dependence of $S(Q,\omega)$ at smaller wave vectors ($Q \lesssim 0.5$ Å$^{-1}$) is not so precisely determined. For $0.2 \lesssim Q \leq 0.5$ Å$^{-1}$, Woods[23] and Cowley and Woods[24] observed that the one-phonon line shape changed little on passing from the superfluid to the normal phase. The phonon linewidths increased sharply with $T$ for $T$ just below $T_\lambda$, but they continued to increase with $T$ for $T > T_\lambda$. These observations are in marked contrast to the temperature dependence at larger wave vectors. Is this a real effect in which $S(Q,\omega)$ for $Q \lesssim 0.5$ Å is similar in the two phases, while at higher $Q$, $S(Q,\omega)$ is quite different?

Since the measurements of Cowley and Woods,[24] there have been significant improvements in signal intensity and instrumental resolution which permit a more precise determination of $S(Q,\omega)$, especially of the linewidth. Our purpose here is to present new data at $Q=0.4$ Å$^{-1}$ and to explore the temperature dependence of $S(Q,\omega)$ and the Woods-Svensson[20] decomposition. We also present new precise data at the roton wave vector $Q=1.935$ Å$^{-1}$ for comparison.

The experiment and analysis of data are discussed in Secs. II and III. The results for $Q=0.4$ and 1.935 Å$^{-1}$ are presented in Secs. IV and V. The data are discussed and compared with theory in Sec. VI.

## II. EXPERIMENTAL DETAILS

The measurements of the dynamic form factor discussed here were made using the IN12 cold-neutron triple-axis crystal spectrometer at the high-flux reactor of the Institute Laue-Langevin (ILL), Grenoble, France. This instrument is situated on a neutron guide tube from the ILL vertical cold source and thus has an enhanced flux of long-wavelength neutrons. Pyrolytic graphite (002) was used as a monochromator and analyzer for all experiments, with a cooled beryllium filter to remove higher-order neutrons. Because of the different energy and wave vector ranges of the two series of measurements, two different experimental configurations were employed. For the $Q=0.4$ Å$^{-1}$ experiments (and some less complete determinations of $Q=0.3$ Å$^{-1}$), the instrument was operated with a fixed *final* neutron energy of 1.127 THz (1 THz=4.135 meV=47.99 K). Collimation of 60′:60′:60′ was used since the neutron intensity is low, even on a high-flux instrument. With these conditions the experimental (incoherent scattering) resolution [full width at half-maximum (FWHM)] was 0.036 THz (1.73 K) and the phonon linewidth (measured FWHM) at the lowest temperature (1.35 K) was 0.044 THz (2.11 K). The order-of-magnitude larger roton structure factor permitted higher instrumental resolution; 30′ collimation was used throughout, with a fixed *incident* energy of 0.913 THz. In this configuration the experimental roton linewidth (FWHM) at 1.23 K was 0.015 THz (0.72 K).

The high-purity $^4$He sample (of volume approximately 40 cm$^3$) was condensed into an aluminum cell of a diameter of 3 cm containing vertically spaced cadmium discs, 1 cm apart, to minimize multiple scattering effects. The sample cell was cooled in a helium flow cryostat and the sample temperature measured by a calibrated carbon resistor. "Empty-cell" measurements were made at each wave vector at the lowest temperatures investigated. In Fig. 1 we present an example of the "full" and "empty"

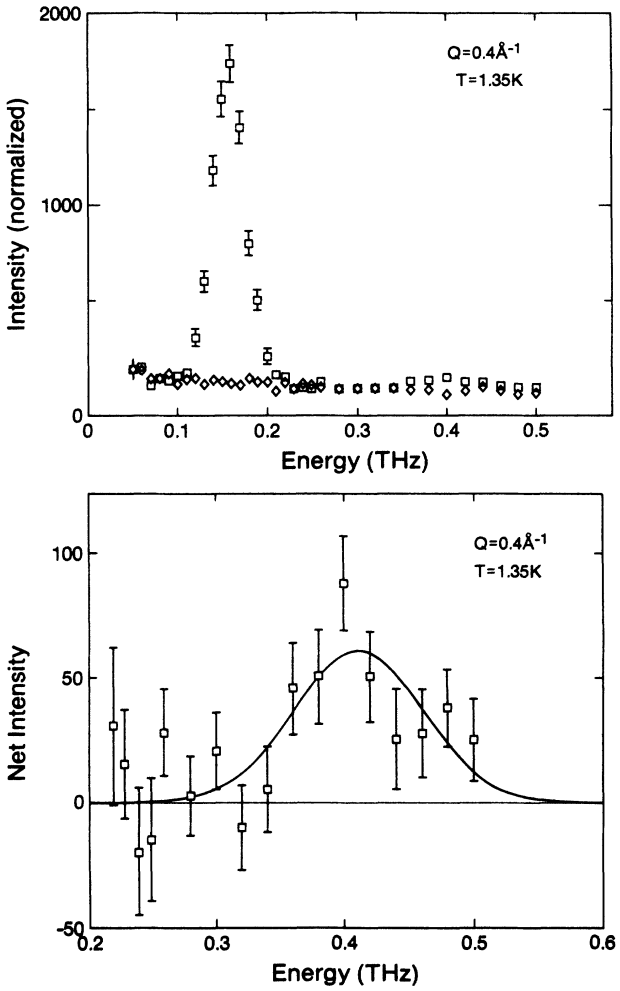


FIG. 1. Upper: empty-cell (◇) and liquid $^4$He plus cell (□) inelastic spectrum for the phonon wave vector ($Q=0.4$ Å$^{-1}$, $T=1.35$ K). Lower: expanded view of multiphonon peak after subtraction of the cell scattering. The solid line is a Gaussian fit as described in the text.

spectra for the phonon wave vector $Q=0.4$ Å$^{-1}$. As is seen in Fig. 1, the inelastic spectrum is dominated by the sharp one-phonon peak at 0.16 THz, with a much weaker broad multiphonon peak at 0.41 THz; this latter feature is shown with the empty-cell scattering subtracted on an expanded scale in Fig. 1.

There is, in fact, little published data on the complete scattering function (one-phonon peak plus, at higher energies, the multiphonon continuum) at small wave vectors, other than that of Svensson *et al.*[21] for $Q=0.3$ Å$^{-1}$. In the present study, therefore, the widest energy range that was kinematically possible was investigated at small wave vectors. The present roton study concentrated on the peak, the dominant feature of the inelastic spectrum, since a wide range of $\omega$ has been observed by Woods and Svensson.[20] At this wave vector the empty-cell scattering was very weak and flat over the range of the measurement.

## III. DATA ANALYSIS

The empty-cell scattering was firstly subtracted from the full spectra to give the net $^4$He scattering. Examples of the resulting helium spectra are shown in Figs. 2 and 3.

To determine the instrumental resolution width, it was assumed that the intrinsic width of the one-phonon (roton) line at $T=1.35$ K ($T=1.23$ K) was negligible. For example, at $Q=0.4$ Å$^{-1}$ and $T=1.35$ K the intrinsic half-width at half-maximum (HWHM) of the one-phonon line measured by Mezei and Stirling[25] using neutron spin echo techniques is approximately $0.8\times10^{-3}$ THz. The observed width here therefore represents the instrument resolution width.

The one-phonon (roton) line at $T=1.35$ K ($T=1.23$ K) was fitted by least squares to a Gaussian function (taken to represent the instrumental resolution function) taking account of the charging analyzer resolution, where appropriate. The fitted functions are shown as the lines of Figs. 2 and 3. This procedure yielded energies and full widths of 0.161 (±0.001) and 0.044 (±0.002) THz for $Q=0.4$ Å$^{-1}$, and 0.179 (±0.0005) and 0.0153 (±0.0013) THz for $Q=1.925$ Å$^{-1}$. These Gaussians were used as the instrumental resolution functions at all higher temperatures.

The dynamic form factor was expressed as a sum of a one-phonon part $S(Q,\omega)$ plus a multiphonon part[26]

$$S(Q,\omega)=S_1(Q,\omega)+S_M(Q,\omega)\ ,$$

in which $S_M(Q,\omega)$ contains any possible interference terms[21] between the one and multiphonon components. The one-phonon scattering function $S_1(Q,\omega)$ was represented, as in the work of Talbot *et al.*,[22] by a Lorentzian function at both positive (neutron energy loss) and negative (neutron energy gain) excitation energies. $S_1(Q,\omega)$ is then written as

$$S_1(Q,\omega)=\frac{1}{2\pi}[n_B(\omega)+1]Z(Q,T)A_1(Q,\omega)\ , \tag{1}$$

where

$$A_1(Q,\omega)=2\left[\frac{\Gamma(Q,T)}{[\omega-\omega(Q,T)]^2+\Gamma(Q,T)^2}-\frac{\Gamma(Q,T)}{[\omega+\omega(Q,T)]^2+\Gamma(Q,T)^2}\right] \tag{2}$$

is the corresponding one-phonon response function. Here $n_B(\omega)$ is the Bose factor for temperature $T$ and frequency $\omega$, $Z(Q,T)$ is the one-phonon intensity, and $\Gamma(Q,T)$ is the HWHM. This choice of analytic form for $S_1(Q,\omega)$ is discussed in detail in Ref. 22 and is expected to be valid when $\Gamma(Q,T)$ is sufficiently small that the full frequency-dependent $\Gamma(Q,\omega,T)$ and $\omega(Q,\omega,T)$ can be

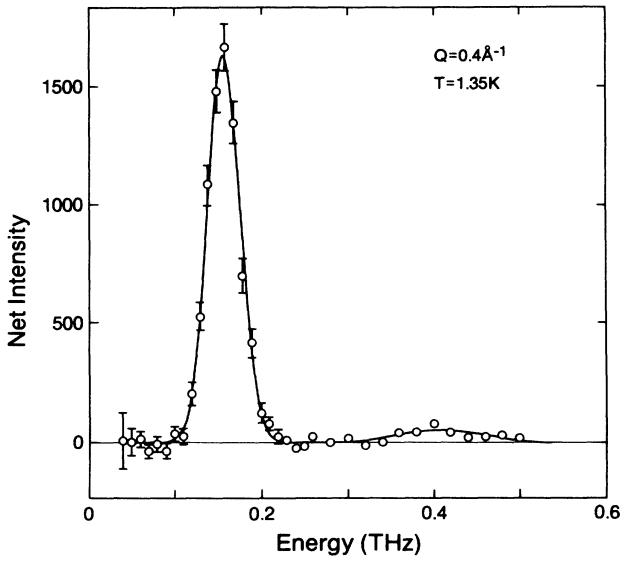


FIG. 2. Net $^4$He scattering after subtraction of empty-cell scattering ($Q=0.4$ Å$^{-1}$, $T=1.35$ K). The solid line is the result of a least-squares fit to two Gaussians as described in the text.

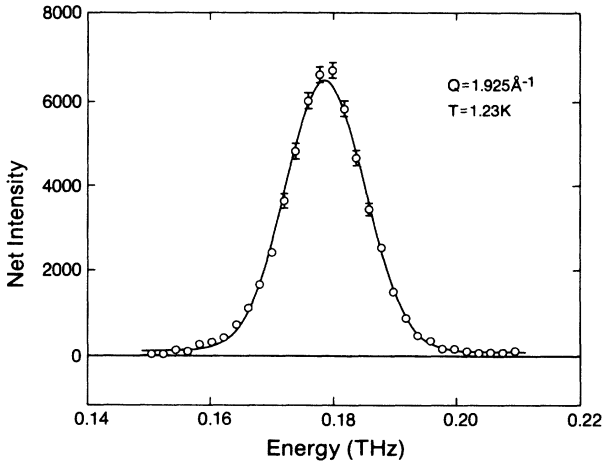


FIG. 3. Net $^4$He scattering at the roton wave vector ($Q=1.925$ Å$^{-1}$, $T=1.23$ K). The solid line represents a Gaussian fit.

well approximated by their on energy shell values [e.g., $\Gamma(Q,\omega,T)\approx\Gamma(Q,T)$ at all $\omega$]. By combining the Lorentzians, $A_1(Q,\omega)$ can be written in the "harmonic oscillator" function form often used to describe phonon response functions.[22] Thus the "Lorentzian" and harmonic oscillator functions are equivalent provided $\omega(Q,T)$ is interpreted as the phonon frequency in each case and not the sum $[\omega^2(Q,T)+\Gamma^2(Q,T)]^{1/2}$. The functions defined in Eqs. (1) and (2) were convoluted with a Gaussian (instrumental resolution) function of unit area and FWHM defined by the lowest temperature data, as described above, and were fitted to the helium data.

For the phonon data, the multiphonon component $S_M(Q,\omega)$ was modeled by a normalized Gaussian function $G_M(Q,\omega)$ with peak height scaled by the appropriate temperature factor of Eq. (1), $S_M(Q,\omega)=[n_B(\omega)+1]G_M(Q,\omega)$. Since the width of $G_M(Q,\omega)$ was large, instrument resolution effects were not removed.

In practice, the final fitted one-phonon parameters were only weakly dependent on the particular form used to describe the multiphoton continuum. For the roton data the weak multiphoton scattering was considered as a small temperature-independent "background"; this simplification has little effect on the one-phonon parameters extracted by the fitting procedure. The fit of $S_M(Q,\omega)$ to the multiphonon scattering at $Q=0.4$ Å$^{-1}$ is shown in Fig. 1.

## IV. PHONON RESULTS ($Q=0.4$ Å$^{-1}$)

Although the bulk of the phonon data was determined at a wave vector of 0.4 Å$^{-1}$, a few measurements were also made at 0.3 Å$^{-1}$. Results for temperatures of 1.35 and 2.96 K at $Q=0.3$ Å$^{-1}$ are displayed in Fig. 4 where the large line broadening at the higher temperature is clearly apparent.

Figures 5 and 6 summarize the inelastic scattering results for $Q=0.4$ Å$^{-1}$. As the temperature is raised, the phonon line broadens and its peak intensity is reduced, while the peak position remains essentially constant.

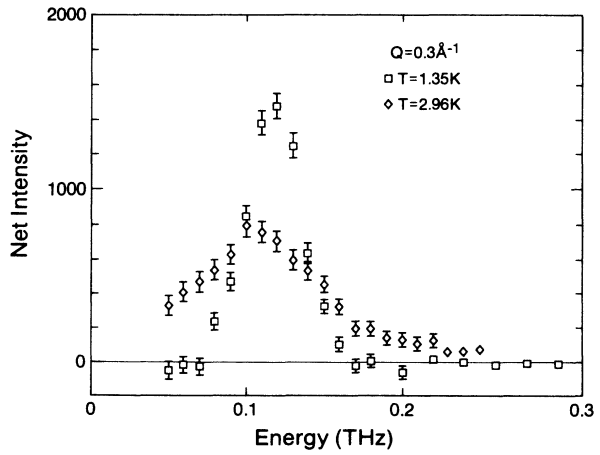


FIG. 4. Comparison of superfluid ($T=1.35$ K) and normal fluid ($T=2.96$ K) spectra for $Q=0.3$ Å$^{-1}$.

The full lines in Figs. 5 and 6 represent the "best-fit" convolutions of Gaussian and Lorentzian functions as described above in Sec. III. The simple Gaussian model for the multiphonon continuum peak introduced in Sec. III describes this part of the spectrum rather well, except at the highest temperature (3.94 K) where multiphonon scattering has largely disappeared as a contribution distinguishable from $S_1(Q,\omega)$. Taken overall, the fit of the simple two-component model to the observed spectra is very satisfactory.

The phonon parameters obtained in this manner are presented in Fig. 7. The phonon frequency is seen to be largely independent of temperature, although there may be a slight increase just below $T_\lambda$. At about 4 K there is an apparent "softening" (somewhat exaggerated by the suppressed zero of the lower frame of Fig. 7); inspection of Fig. 6 suggests that this is indeed a real effect as there is a significant shift of intensity to lower frequency between 3 and 4 K. The half-width at half-maximum $\Gamma$ of $A_1(Q,\omega)$ increases smoothly through the $\lambda$ point with little sign of any discontinuity, although the rate of increase decreases above the transition. We note that a small systematic error is introduced in our analysis since we have used the 1.35-K linewidth as a measure of the instrumental broadening. However, the work of Mezei and Stirling,[25] which concentrated on temperatures below 1.7 K, has shown that the HWHM at 1.35 K for the wave vector considered is less than 0.001 THz, producing a negligible effect on the phonon widths extracted. Finally, Fig. 7 shows that the one-phonon intensity also shows little evidence for a discontinuity at the $\lambda$ point. So there is indeed little evidence for a qualitative change in the form of $S(Q,\omega)$ at or near the $\lambda$ point. To further support this contention, we compare spectra just below (2.04 K) and just above $T$ (2.32 K) in Fig. 8. The only significant difference is in the peak intensity, while there is a slight shift to higher frequency just above $T_\lambda$ as seen also in Fig. 7.

Above the $\lambda$ point the spectra at 2.24, 2.32, 2.56, and 2.96, are similar, except for a slight increase in width with temperature and some increase in scatter of the data in the peak region with temperature. The similarity is displayed in Fig. 9 where a low temperature spectrum is included for comparison. As noted, the $T=3.94$ K spectrum is significantly displaced toward lower frequency.

In the Woods-Svensson[20] (WS) model, $S(Q,\omega)$ is expressed as a sum of a superfluid and normal component

$$S(Q,\omega)=\frac{\rho_S(T)}{\rho}S_S(Q,\omega)+\frac{\rho_N(T)}{\rho}S_N(Q,\omega)\ . \qquad (3)$$

In the normal phase where $\rho_N=\rho$, $S(Q,\omega)$ reduces to $S_N(Q,\omega)$. To explore the WS model for $Q=0.4$ Å$^{-1}$, we determined $S_N(Q,\omega)$ as $S_N(Q,\omega)=S(Q,\omega)$ for $T=2.32$ K. We denote this as $S_N^*(Q,\omega)$. In the superfluid phase where both components of $S(Q,\omega)$ contribute, we determined $[\rho_S(T)/\rho]S_S(Q,\omega)$ as

$$[\rho_S(T)/\rho]S_S(Q,\omega)\equiv S(Q,\omega)-\frac{\rho_N(T)}{\rho}S_N^*(Q,\omega)$$
$$=S_1(Q,\omega)-\frac{\rho_N(T)}{\rho}S_1^*(Q,\omega)+\left\{[n_B(\omega)+1]-\frac{\rho_N(T)}{\rho}[n_B^*(\omega)+1]\right\}G_M(Q,\omega)\ , \tag{4}$$

where we have used $S(Q,\omega)=S_1(Q,\omega)+S_M(Q,\omega)$ and $S_M(Q,\omega)=[n_B(\omega)+1]G_M(Q,\omega)$. The $S_S(Q,\omega)$ determined in this way is dominated by the one-phonon parts of $S(Q,\omega)$. In the $\omega$ range where $G(Q,\omega)$ is significant, $n_B(\omega)$ and $n_B^*(\omega)$ are negligible so that the second term reduces to $\{1-[\rho_N(T)/\rho]\}G_M(Q,\omega)$. This term serves simply to add a multiphonon component as $T$ decreases below $T_\lambda$, which may or may not be meaningful.

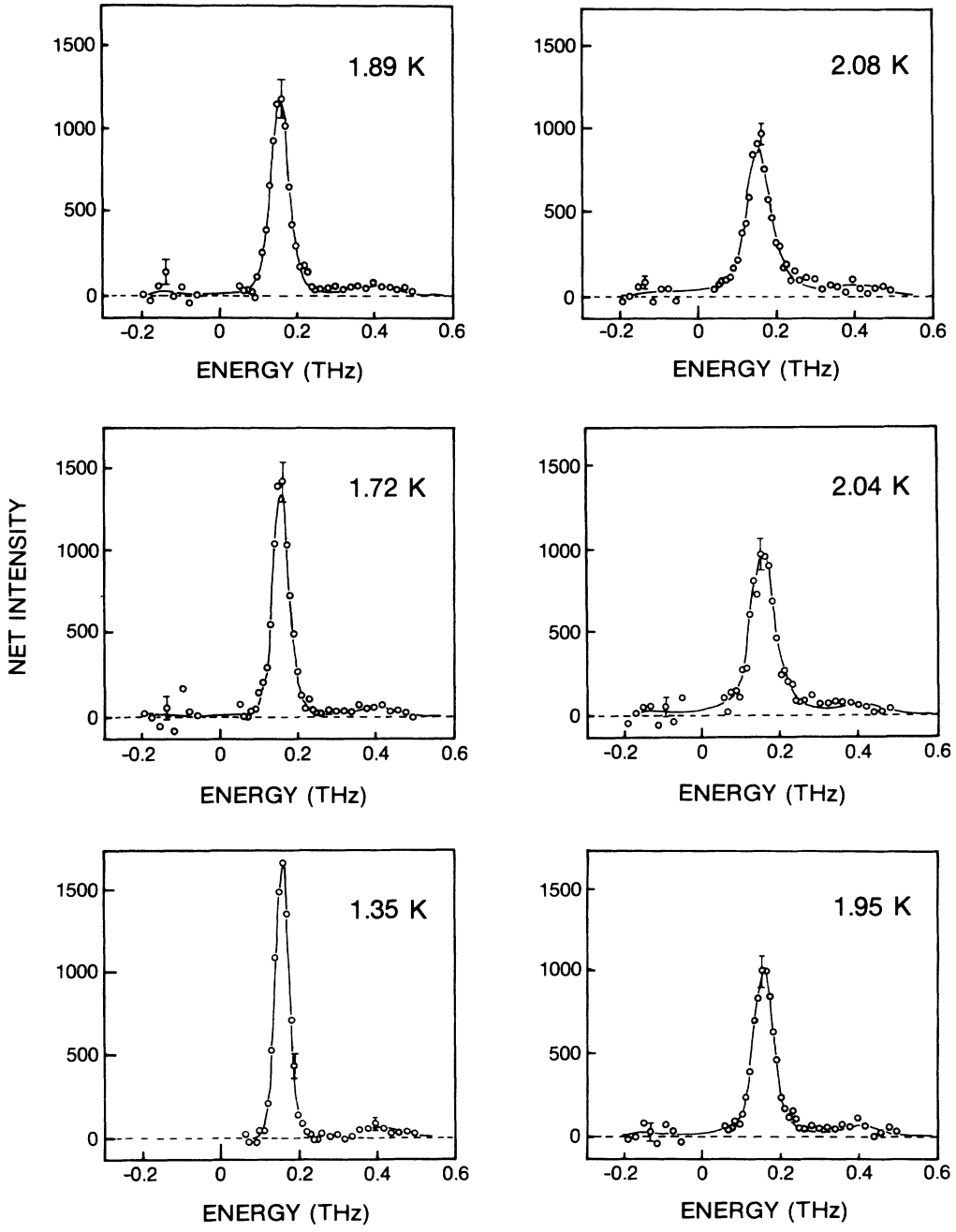


FIG. 5. Temperature dependence of the phonon spectrum ($Q=0.4$ Å$^{-1}$). The solid lines are the fitted Lorentzian convolutions as described in the text.

The resulting instrument resolution broadened $[\rho_S(T)/\rho]S_S(Q,\omega)$ is shown in Fig. 10. For the lowest temperatures the ratio of normal to superfluid densities is relatively small (0.06 for $T=1.35$ K) so $S_S$ is only slightly different from the total $S_1$. At higher temperatures, however, the superfluid component $S_S$ consists of a sharp peak which goes slightly negative in the wings, indicating that too much intensity has been subtracted. Although this effect is small, of the same order of magnitude as the scatter in the low intensity data points, we believe the net negative intensity suggests that $S_S(Q,\omega)$ is not physically meaningful. We have also made the subtraction via the intrinsic $S(Q,\omega)$ (not resolution broadened) using Eq. (4) and the data in Table I and obtained similar negative intensity in the wings. As in our previous study,[22] we find that (3) is not an accurate enough description to have compelling fundamental meaning. In addition, the present data at $Q=0.4$ Å$^{-1}$ do not suggest *a priori* a decomposition of the form (3).

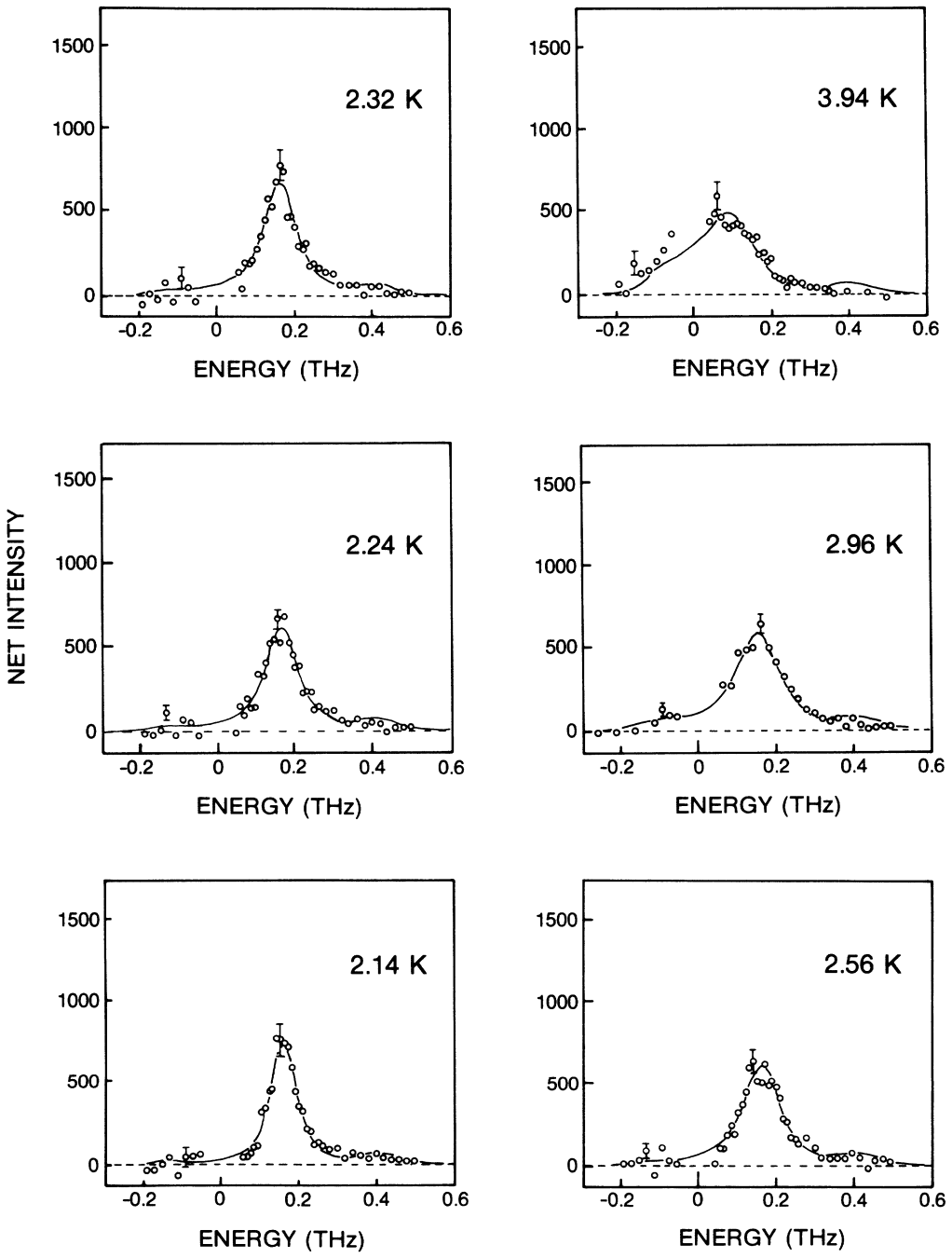


FIG. 6. As Fig. 5.

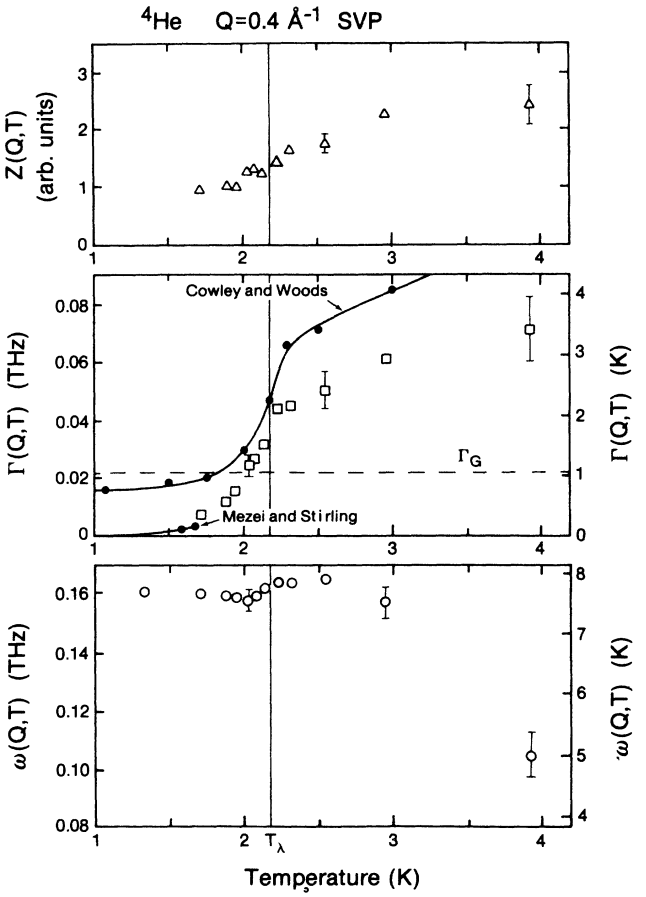


FIG. 7. Fitting parameters $\omega(Q,T)$, $\Gamma(Q,T)$, and $Z(Q,T)$ of Eq. (2) for the phonon spectra ($Q=0.4$ Å$^{-1}$). The dashed line shows the Gaussian resolution width $\Gamma_G$ used in the convolution procedure. The solid lines are previous half-widths at half-maximum [$\Gamma(Q,T)$] observed by Cowley and Woods (Ref. 24) and Mezei and Stirling (Ref. 25).

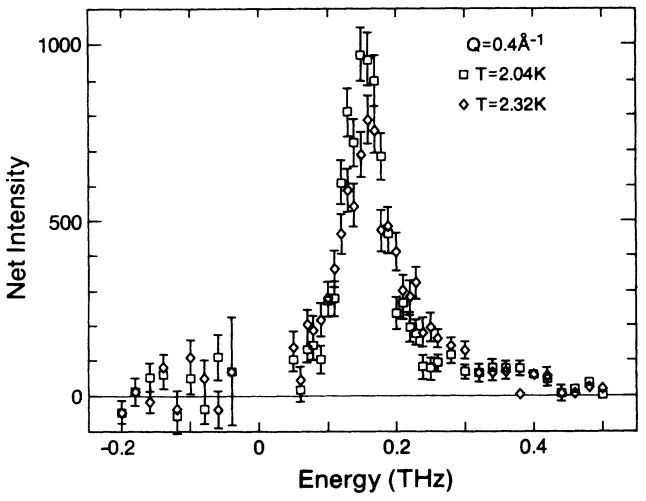


FIG. 8. Comparison of the phonon spectrum ($Q=0.4$ Å$^{-1}$) just below $T_\lambda$ (2.04 K; □) and just above $T_\lambda$ (2.32 K; ◇).

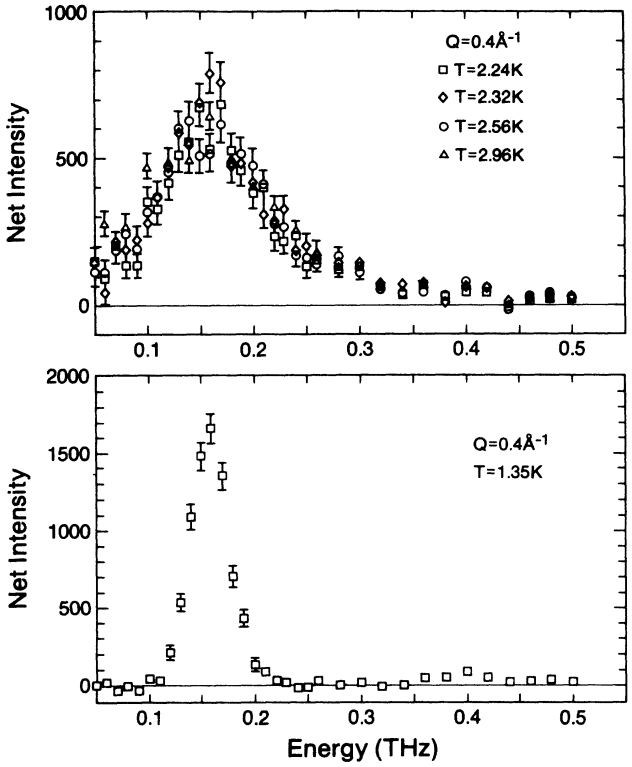


FIG. 9. Comparison of the phonon spectrum ($Q=0.4$ Å$^{-1}$) above $T_\lambda$, with the lowest temperature ($T=1.35$ K) result.

## V. ROTON RESULTS ($Q=1.925$ Å$^{-1}$)

The observed scattering intensity at the roton wave vector is displayed in Figs. 11 and 12. The solid lines are fits of Eqs. (1) and (2) to the data convoluted with a Gaussian to represent the instrument resolution as discussed in Sec. III.

As observed in previous studies, the roton linewidth increases and the roton peak intensity drops rapidly with increasing $T$ for $T<T_\lambda$. The increase in the linewidth is particularly rapid in the temperature range just below $T_\lambda$. The rapid change in character of the scattered intensity just below $T_\lambda$ is displayed in Fig. 13 where the scattered intensity at $T=1.79$, 2.02, 2.09, and 2.17 K are compared. It is clear that there is a qualitative change in the inelastic spectrum between 2.09 and 2.17 K. In the superfluid phase there remains an identifiable peak in the scattered intensity which has disappeared at $T_\lambda$. Above $T_\lambda$ there is relatively little change in the shape of the observed scattering intensity with temperature, although the frequency $\omega(Q,T)$ decreases significantly and the linewidth $\Gamma(Q,T)$ continues to increase as $T$ is increased above $T_\lambda$. The similarity of the observed intensity at all temperatures in the normal phase above $T_\lambda$ is displayed in Fig. 14, where the spectra at 2.33, 2.48, and 2.96 K are compared. In general, the shape of the scattered intensity is quite different in the superfluid and normal phases, particularly in its temperature dependence.

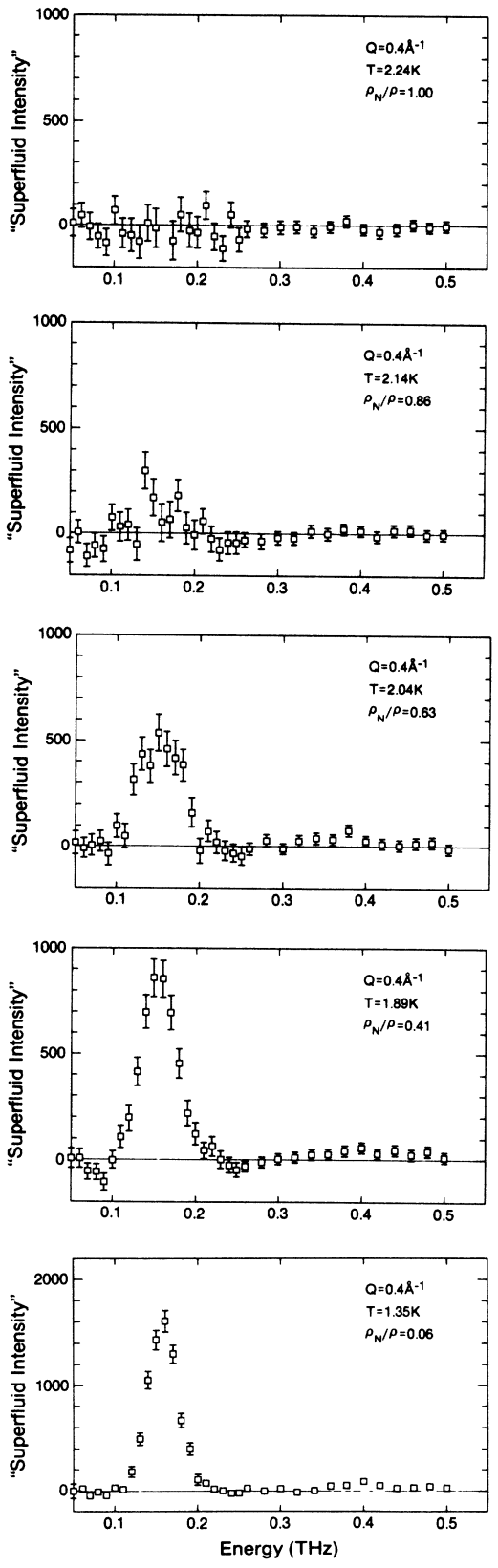


FIG. 10. Resolution broadened values of $\rho_S(T)/\rho)S_S(Q,\omega)$ obtained by subtracting a "normal fluid component" from the superfluid phase phonon spectra ($Q=0.4$ Å$^{-1}$), as described in the text.

As seen from Figs. 11 and 12, the fitted $S_1(Q,\omega)$ of Eqs. (1) and (2) provide a very satisfactory description of the temperature dependence of the scattering intensity. A *single* Lorentzian function was also fitted to the data and, while providing a reasonable fit at low and high temperatures, this form was unsatisfactory between 1.93 and 2.33 K. The roton parameters $Z(Q,T)$, $\omega(Q,T)$, and $\Gamma(Q,T)$ obtained using Eqs. (1) and (2) are shown in Fig. 15. The $\omega(Q,T)$ and $\Gamma(Q,T)$ reported here agree well with previous measurements. For example, the roton HWHM at 1.37 K found here is 0.1 K, while Mezei[27] reports 0.11 K at $T=1.4$ K. Comparing Fig. 7 and Fig. 15 we see that the roton linewidth increases significantly more rapidly with temperature than does the phonon linewidth. Indeed, at $T_\lambda$ and above, the spectral linewidth at $Q=1.925$ Å$^{-1}$ is approximately three times greater than the linewidth at $Q=0.4$ Å$^{-1}$, whereas at $T\approx 1$ K both lines are extremely narrow. Below $T_\lambda$ the roton $\omega(Q,T)$ also decreases with increasing $T$ (a frequency shift $\Delta=[\omega(Q,T)-\omega(Q,T=0\ \text{K})]\propto\rho_N(T)$) (Refs. 19 and 27), while the phonon $\omega(Q,T)$ is essentially independent of $T$. In the normal phase the temperature dependence of $\omega(Q,T)$ at $Q=1.925$ and 0.4 Å$^{-1}$ is quite different. In particular, at $Q=0.4$ Å$^{-1}$ the ratio of $\Gamma(Q,T)/\omega(Q,T)$ in the normal phase is sufficiently small that the scattered intensity can reasonably be attributed to a single collective excitation. This is not the case at the roton wave vector.

## VI. DISCUSSION AND INTERPRETATION

### A. Energies and lifetimes

To obtain the energies $\omega(Q)$ and inverse lifetimes $\Gamma(Q)$ we fitted the response function $A_1(Q,\omega)$ in (2) to the intrinsic one-phonon part of the data. This $A_1(Q,\omega)$ is the exact response function[10] for a boson (a Bose quasiparticle or phonon) in which the self energy $\Sigma(Q,\omega)=\Delta(Q,\omega)-i\Gamma(Q,\omega)$ is approximated by its "on-shell" value $\Sigma(Q,\omega)\approx\Sigma[Q,\omega(Q)]$. In this approximation, $\Sigma$ becomes independent of frequency and the full[10] $A_1(Q,\omega)$ reduces to (2) in which $\omega(Q)=\omega^0(Q)+\Delta[Q,\omega(Q)]$, $\Gamma(Q)=\Gamma[Q,\omega(Q)]$, and $\omega^0(Q)$ is the noninteracting boson energy.

By combining the two Lorentzians in (2), $A_1(Q,\omega)$ takes the form

$$A_1(Q,\omega)=\frac{8\omega\Gamma(Q)\omega(Q)}{\{\omega^2-[\omega^2(Q)+\Gamma^2(Q)]\}^2+4\omega^2\Gamma(Q)^2}\ . \tag{5}$$

Equation (5) is often referred to as the harmonic oscillator (HO) function.[28] The Lorentzian (2), which has a Stokes and anti-Stokes term, is clearly the same as the HO function. However, in using (5) the sum $E^2(Q)=\omega^2(Q)+\Gamma^2(Q)$ is often interpreted as the phonon energy. The relation $E^2(Q)=\omega^2(Q)+\Gamma^2(Q)$ may be used to relate the present $\omega(Q)$ in Table I to the values $E(Q)$ quoted by Tarvin and Passell[28] for the roton energy. Given the fundamental nature of (2), we believe $\omega(Q)$ is the most appropriate energy. However, when $S(Q,\omega)$ is very broad and $A_1(Q,\omega)$ is needed over a wide range of $\omega$, defining a frequency-independent $\omega(Q)$ and $\Gamma(Q)$ may

not be meaningful.

The present half-width $\Gamma(Q)$ at $Q=0.4$ Å$^{-1}$ is compared with the values quoted by Cowley and Woods[24] and by Mezei and Stirling[25] in Fig. 7. The values quoted by Cowley and Woods[24] include the instrument resolution and are therefore larger than the present values. The present values at low $T$ are larger than those quoted by Mezei and Stirling.[25] We believe this is because the present instrument resolution $\Gamma_G$ is much larger than the intrinsic $\Gamma(Q)$ at low $T$, which makes is difficult to extract a small $\Gamma(Q)$ with precision. At low $T$ the Mezei and Stirling values are more reliable.

In Fig. 16 we compare the present $\Gamma(Q)$ for the roton with those obtained by Woods and Svensson[20] At SVP and by Talbot *et al.*[22] at 20 bar pressure. The present $\Gamma(Q)$ agree with the WS values at low $T$ but are larger at higher $T$ [$T$ near $T_\lambda$]. The present $\Gamma(Q)$ are larger because we have fitted (2) to the whole of the one-phonon

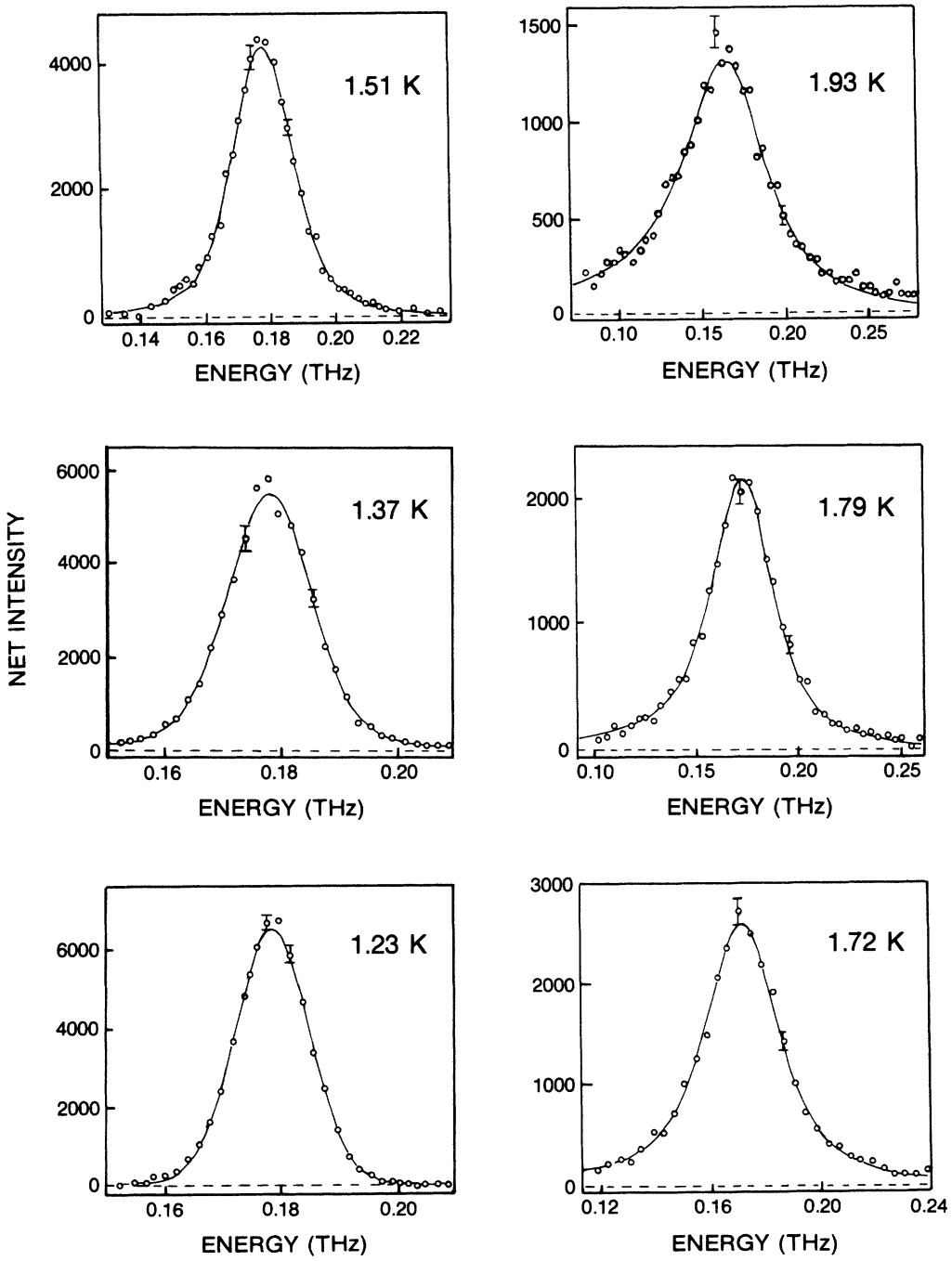


FIG. 11. Temperature dependence of the roton spectrum ($Q=0.1925$ Å$^{-1}$). The solid lines are the fitted Lorentzian convoutions as described in the text.

peak rather than that part of it identified by WS as the one-phonon peak in the superfluid component of $S(Q,\omega)$. The present analysis is similar to the simple subtraction method used by Talbot *et al.*[22] If the interpretation discussed in Sec. VI that the sharp component of $S(Q,\omega)$ for the roton arises from single quasiparticle excitation is indeed correct, then the lifetimes extracted by WS may be a better representation of the quasiparticle lifetime.

### B. Comparison of normal liquid $^4$He with other fluids

To interpret the observed scattering from normal $^4$He we make comparisons with liquid $^3$He, heavier fluids, and solid $^4$He. In Fig. 17 we compare our observed intensity for normal $^4$He in the phonon region ($Q=0.4$ Å$^{-1}$) and $T=2.32$ K with $S(Q,\omega)$ observed in liquid $^3$He at

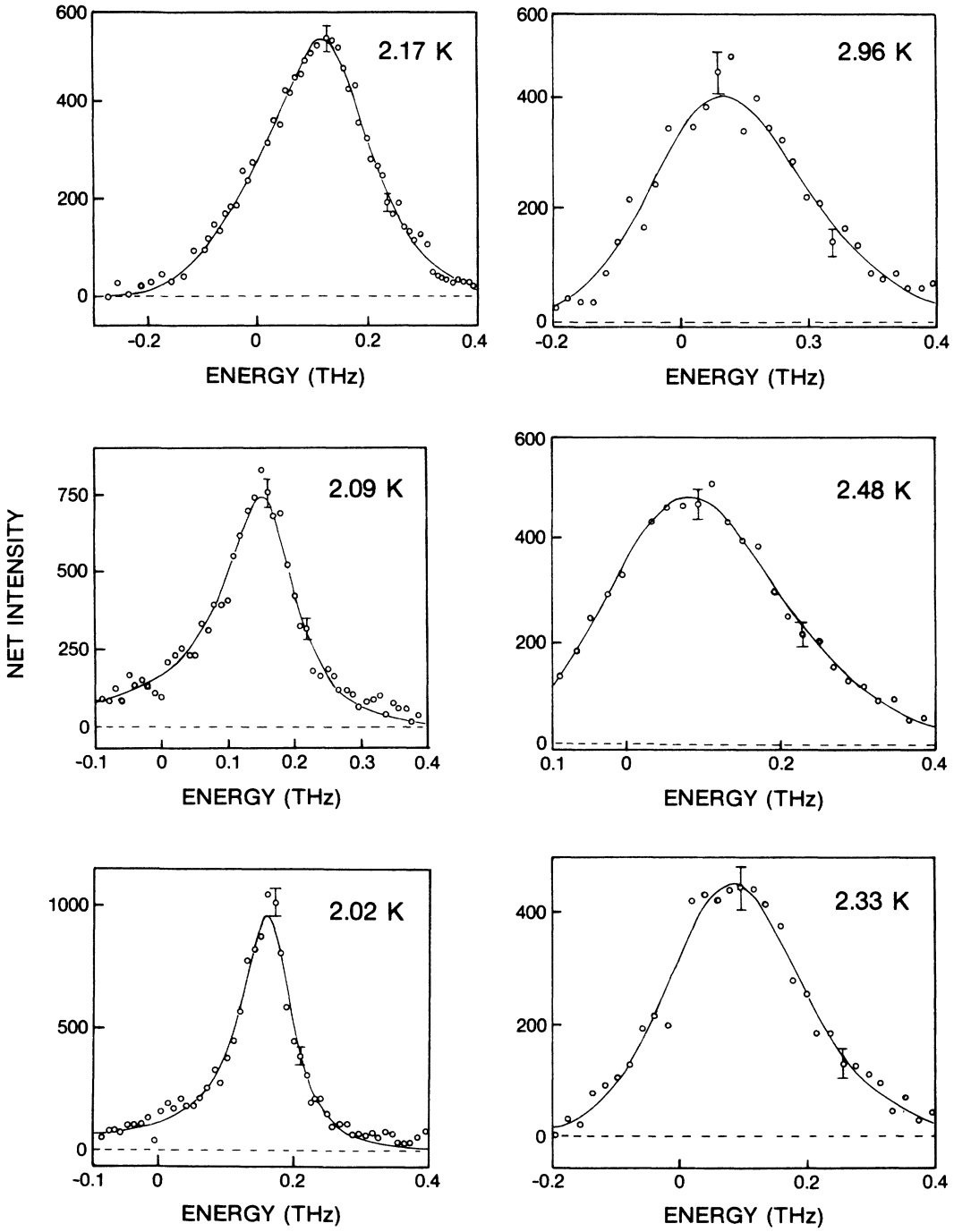


FIG. 12. As Fig. 11.

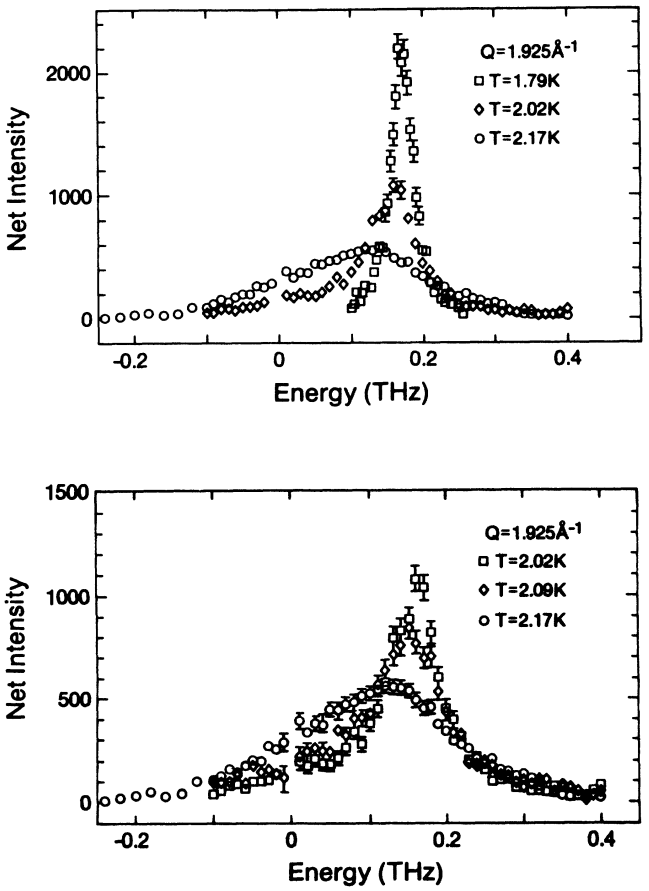


FIG. 13. Comparison of roton spectra ($Q=1.925$ Å$^{-1}$) below $T_\lambda$ and at $T_\lambda$ ($T=2.17$ K). For clarity, some data are presented twice.

$Q=0.5$ Å$^{-1}$ and $T=0.12$ K by Scherm *et al.*[29] The peak in $S(Q,E)$ in liquid $^3$He at $\nu=0.18$ THz is identified as scattering from the collective zero sound (phonon) mode with spin fluctuation scattering at lower $\nu$. The width of the one-phonon peak is similar in the two cases;

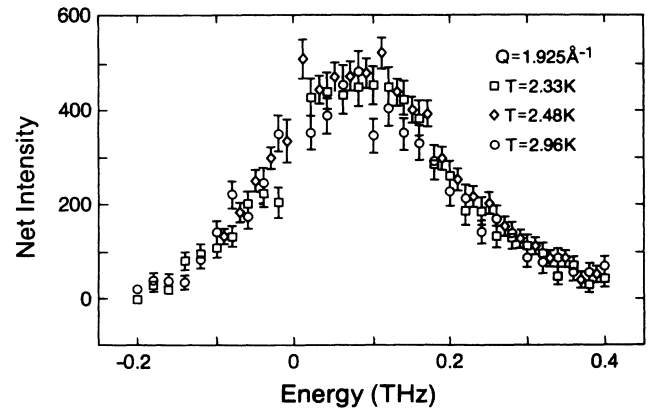


FIG. 14. Comparison of roton spectra ($Q=1.925$ Å$^{-1}$) above $T_\lambda$.

a FWHM$=2\Gamma\approx0.1$ THz for $^4$He and 0.05 THz for $^3$He. Since the peak position[30] and width[31] in $^3$He is quite successfully interpreted as a collective zero sound mode, it is natural to interpret the peak in normal $^4$He in the same way. Liquid Ne supports a well-defined collective density excitation[32] up to $Q=0.16$ Å$^{-1}$ but not[33] for $Q\gtrsim0.8$ Å$^{-1}$. Liquid Rb and other liquid metals support[34–36] a well-defined collective mode at $Q\approx0.3$ Å$^{-1}$ (the FWHM is approximately one-half the peak frequency), but the peak is certainly gone by $Q\approx1.0$ Å$^{-1}$. Historically[1] and on the basis of these comparisons, the peak in $S(Q,\omega)$ in normal $^4$He at $Q=0.4$ Å$^{-1}$ may be interpreted as a collective zero sound mode in the fluid density.

In Fig. 18 we compare the scattering intensity at $Q=1.13$ Å$^{-1}$ (maxon) and at $Q=1.93$ Å$^{-1}$ (roton) from normal $^4$He at $p=20$ bar at several temperatures[22] with $S(Q,\omega)$ observed[36] in liquid $^3$He at $Q=1.2$ and 2.0 Å$^{-1}$.

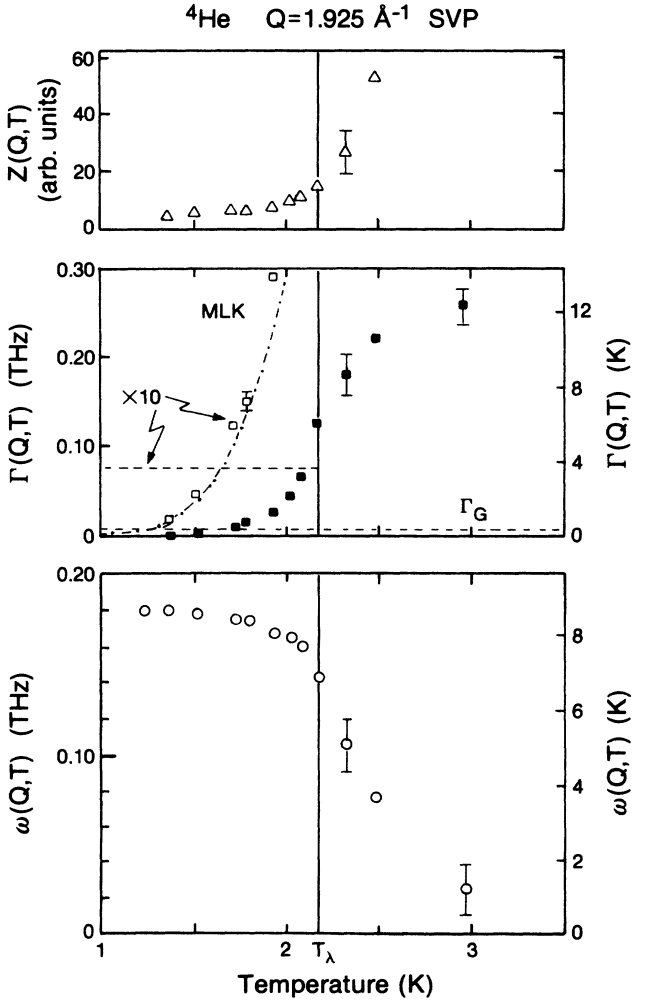


FIG. 15. Fitting parameters $\omega(Q,T)$, $\Gamma(Q,T)$, and $Z(Q,T)$ of Eq. (2) for the roton spectra ($Q=1.925$ Å$^{-1}$). The dashed line shows the Gaussian resolution width used in the deconvolution procedure. Results for the superfluid phase are also displayed multiplied by 10; for comparison results of Mezei (Ref. 27) and Landau and Khalatnikov (Ref. 19) are shown as the dot-dashed line.

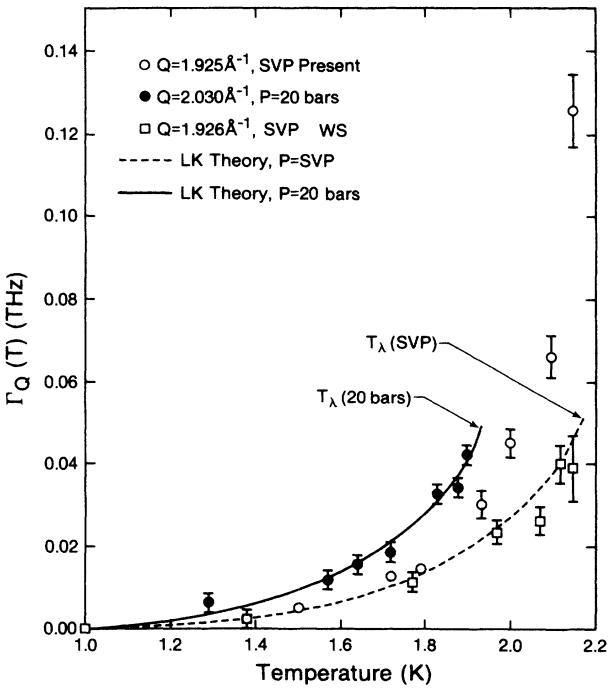


FIG. 16. One-phonon half-widths $\Gamma(Q,T)$ at the roton $Q=1.926$ Å$^{-1}$: open circles with error bar present values obtained by fitting (2) to the whole of the "one-phonon" peak (see text); open squares with error bar represent Woods and Svensson (WS) values (Ref. 20) obtained by fitting to the one-phonon peak showing intensity approximately proportional to $\rho_S(Q,T)$; closed circles with error bar represent values at $p=20$ bar obtained by Talbot *et al.* (Ref. 22) following the WS analysis. Lines are the Landau-Khalatnikov (Ref. 19) theory.

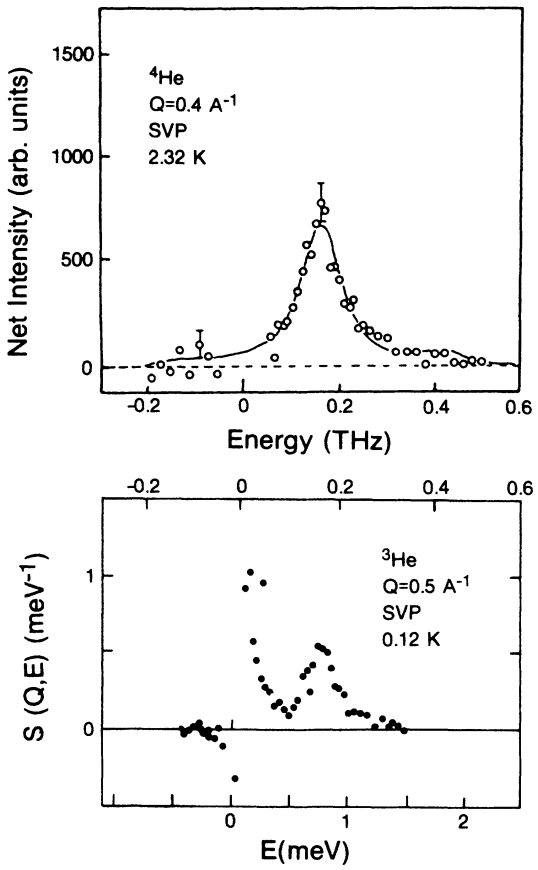


FIG. 17. $S(Q,\omega)$ observed in liquid $^3$He at $Q=0.5$ Å$^{-1}$ (Ref. 29) and in liquid $^4$He at $Q=0.4$ Å$^{-1}$ (present).

The intensity observed in normal liquid $^4$He is largely temperature independent. In liquid $^3$He between $T=40$ mK and 1.2 K, $S(Q,\omega)$ also differs little. Thus in normal $^4$He and liquid $^3$He, $S(Q,\omega)$ is largely independent of temperature. In $^3$He there is no collective excitation for $Q \gtrsim 1.2$ Å$^{-1}$. Rather, $S(Q,\omega)$ represents broad scattering from particle-hole excitations. The scattering observed at $Q=1.13$ Å$^{-1}$ in normal liquid $^4$He is broader than $S(Q,\omega)$ in $^3$He (i.e., FWHM$\approx$0.6 THz in $^4$He compared with FWHM$\approx$0.4 THz in $^3$He). To set the scale, the zero sound mode width at $Q=1$ Å$^{-1}$ in $^3$He is $2\Gamma\approx 0.2$ THz and the width of a typical longitudinal phonon midway in the Brillouin zone of bcc $^4$He ($p\approx 25$ bar) is $2\Gamma\approx 0.25$ THz.[1] These comparisons suggest strongly that normal $^4$He does not support a collective excitation at $Q\approx 1.1$ Å$^{-1}$. Rather, $S(Q,\omega)$ at $Q\approx 1.13$ Å$^{-1}$ in normal $^4$He represents scattering from pairs of single-particle excitations. Also, the data of Woods and Svensson[20] and of Talbot *et al.*[22] for $T<T_\lambda$, reproduced here in Fig. 19, suggest that the sharp peak in $S(Q,\omega)$ in the superfluid phase disappears at $T=T_\lambda$ leaving only broad scattering. The situation is similar but not so clear at the roton wave vector, chiefly because the roton energy is so small. However, there is probably no collective mode in normal $^4$He at the roton wave vector. On the basis of their data and comparison with other fluids, Pederson and Carneiro[28] also suggest there is no collective excitation in normal $^4$He at the roton $Q$.

### C. Some speculative remarks

The present data at $Q=0.4$ Å$^{-1}$ and previous data for $Q\gtrsim 1.1$ Å$^{-1}$ show that the temperature dependence of $S(Q,\omega)$ is quite different at these two $Q$ values. At $Q\lesssim 0.4$ Å$^{-1}$, the peak in $S(Q,\omega)$ broadens gradually with increasing $T$, but has the same basic shape in the superfluid and normal phases. In the normal phase, the peak remains well defined as expected for a collective density mode. At $Q\geq 1.1$ Å$^{-1}$ the sharp peak in $S(Q,\omega)$, seen in the superfluid phase, apparently disappears at $T_\lambda$. In the normal phase, $S(Q,\omega)$ is very broad, which is characteristic of scattering from pairs (or high multiples) of quasiparticles and no collective mode. We make some speculative remarks relating this behavior to microscopic theories of liquid $^4$He.

Landau,[2] and Feynman and Cohen[3] proposed that superfluid $^4$He supports a collective excitation in the fluid density $\rho(r)=\int dr\, e^{iQr}\rho(Q)$. This excitation appears as the sharp component in $S(Q,\omega)$,

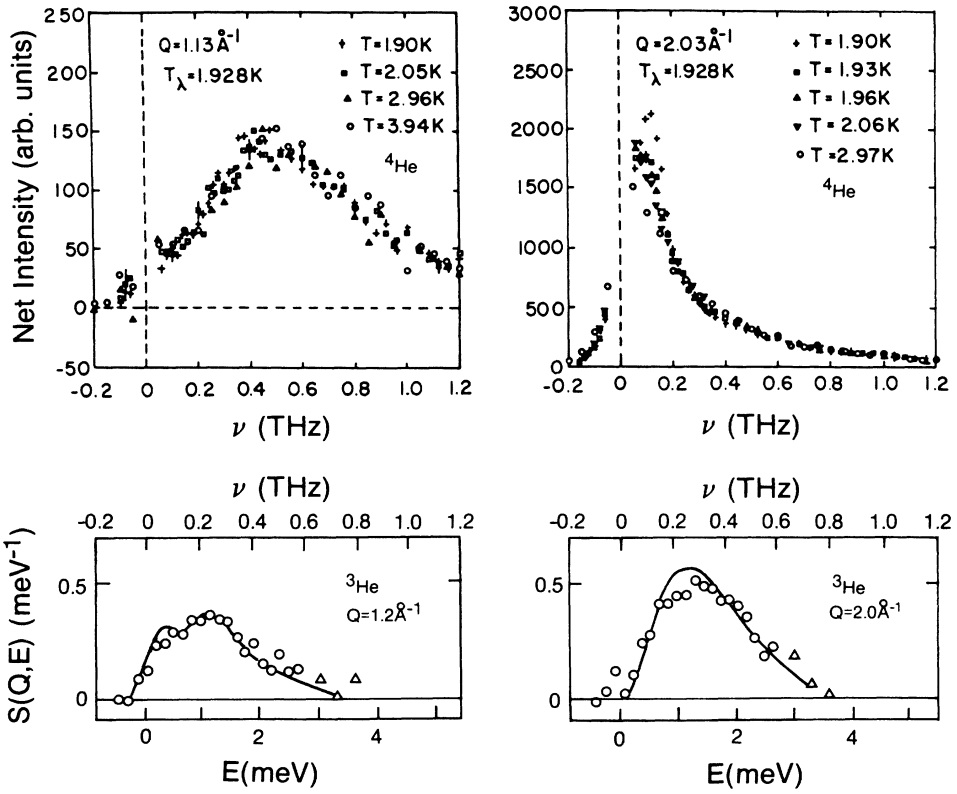


FIG. 18. Upper: scattered intensity from liquid $^4$He at $Q=1.13$ Å$^{-1}$ (maxon) and $Q=2.03$ Å$^{-1}$ (roton) (Ref. 22) for temperatures near $T_\lambda$ and above. Lower: $S(Q,\omega)$ of liquid $^3$He at $Q=1.2$ and 2.0 Å$^{-1}$; $T=40$ mK (solid line) and $T=1.2$ K (open circles) (Ref. 36).

TABLE I. One-phonon parameters appearing in the response function $A_1(Q,\omega)$ of Eq. (2) at the phonon ($Q=0.4$ Å$^{-1}$) and roton ($Q=1.925$ Å$^{-1}$) wave vectors.

| $T$ | $\omega(Q,T)$ (THz) | $\Gamma(Q,T)$ (THz) | $Z(Q,T)$ (arb. units) |
|---|---|---|---|
| | Phonon ($Q=0.4$ Å$^{-1}$) | | |
| 1.35 | 0.161±0.001 | | |
| 1.72 | 0.161±0.0015 | 0.007(4)±0.002 | 2.97±0.09 |
| 1.89 | 0.160 | 0.011(1) | 3.22 |
| 1.95 | 0.159 | 0.015(0) | 3.26 |
| 2.04 | 0.159 | 0.023(6) | 4.04 |
| 2.08 | 0.160 | 0.026(9) | 4.13 |
| 2.14 | 0.163 | 0.031(4) | 4.00 |
| 2.24 | 0.165±0.004 | 0.043(8)±0.006 | 4.52±0.30 |
| 2.32 | 0.164 | 0.045(0) | 5.14 |
| 2.56 | 0.165 | 0.049(4) | 5.49 |
| 2.95 | 0.157 | 0.061(0) | 7.21 |
| 3.94 | 0.105±0.008 | 0.070(6)±0.011 | 7.56±0.50 |
| | Roton ($Q=1.925$ Å$^{-1}$) | | |
| 1.23 | 0.1789±0.0005 | | |
| 1.37 | 0.1785±0.0005 | 0.002 ±0.003 | 5.70±0.15 |
| 1.51 | 0.1770 | 0.005 | 6.44 |
| 1.72 | 0.1739 | 0.012(5) | 7.60 |
| 1.79 | 0.1734 | 0.0150 | 7.54 |
| 1.93 | 0.1671 | 0.029 | 8.64 |
| 2.02 | 0.1642 | 0.046 | 9.90 |
| 2.09 | 0.1603 | 0.066 | 11.3 |
| 2.17 | 0.1428±0.004 | 0.123 ±0.010 | 16.4 ±1.2 |
| 2.33 | 0.1048 | 0.183 | 26.8 |
| 2.48 | 0.0758 | 0.223 | 54.0 |
| 2.96 | 0.0249±0.015 | 0.26 ±0.02 | 187.2 ±200.0 |

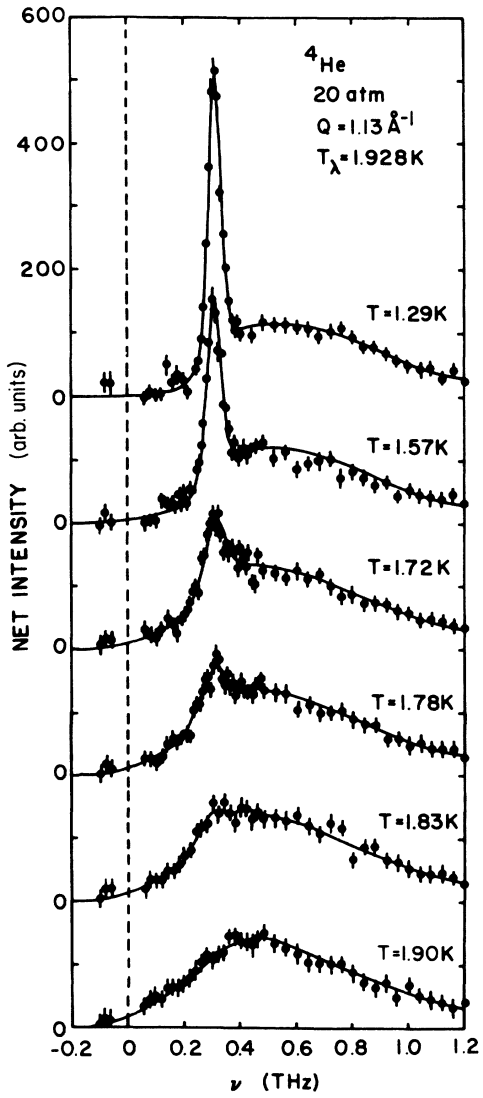


FIG. 19. Temperature dependence of the net scattering intensity from liquid $^4$He at $p=20$ bar and $Q=1.13$ Å$^{-1}$, from Talbot *et al.* (Ref. 22).

$$S(Q,\omega)=\frac{1}{2\pi}\int dt\, e^{i\omega t}\langle \rho(Q,T)\rho^{\dagger}(Q,0)\rangle \ . \tag{6}$$

The corresponding dynamic susceptibility is

$$\chi(Q,t)=-i\langle T\rho(Q,t)\rho^{\dagger}(Q,0)\rangle \ . \tag{7}$$

Here $\rho^{+}(Q)=\sum_k a^{\dagger}_{k+Q}a_k$ is the density creation operator which may be expressed as a coherent sum of particle $(a^{\dagger}_{k+Q})$ and hole $(a_k)$ pair excitations. The collective density excitation follows[2,3] from the strong interaction between the $^4$He atoms and Bose statistics. The temperature dependence of the collective mode was not fully discussed.

Alternatively, Bogolubov,[37] Hugenholtz and Pines,[6] Gavoret and Nozières,[7] and the subsequent dielectric formulation[8–17] present a somewhat different view based on Green's functions.[10] The Bose broken symmetry and the condensate play a central role. Specifically, when there is a macroscopic fraction $N_0$ of the N atoms in the zero momentum state $(k=0)$ $\hat{a}_0$ and $a^{\dagger}_0$ may be replaced by numbers $(a^{\dagger}_0|k=0\rangle=a_0|k=0\rangle=\sqrt{N_0}|k=0\rangle)$. The density operator therefore separates into two parts $\rho(Q)=\sqrt{N_0}(a_Q+a^{\dagger}_{-Q})+\rho'(Q)$, where $\rho'(Q)=\sum'_k a^{\dagger}_k a_{k+Q}$ involves particles above the condensate $(k\neq 0)$ only. Substituting $\rho(Q)$ into (7), and the dynamic susceptibility $\chi$ separates into two parts

$$\chi(Q,\omega)=n_0\sum_{\alpha\beta}\Lambda_\alpha G_{\alpha\beta}(Q,\omega)\Lambda_\beta+\chi'_R(Q,\omega) \ ,$$

where

$$S(Q,\omega)=-\frac{1}{\pi}[n_B(\omega)+1]Im\chi(Q,\omega) \ . \tag{8}$$

Here $n_B(\omega)$ is the Bose function and $n_0=N_0/N$. The singular part $\chi_S=n_0\Lambda G\Lambda$ is proportional to single-particle Green's functions of the form $G_{11}(Q,t)=-i\langle Ta_Q(t)a^{+}_Q(0)\rangle$. This comes from the first term of $\rho(Q)$ and represents excitation of single quasiparticles having momentum $Q$. The regular part is

$$\chi'_R(Q,t)=-i\langle T\rho'(Q,t)\rho'^{\dagger}(Q,0)\rangle \ ,$$

which represents excitation of particle-hole pairs, involving atoms outside the condensate only.

The functions $\Lambda_\alpha(Q,\omega)$ are given by $\Lambda_\alpha(Q,\omega)=[1-P_\alpha(Q,\omega)]$ in which the $P_\alpha(Q,\omega)$ incorporates the interference[38] between scattering, which excites a single particle $(G_{\alpha\beta})$ and pairs of particles $(\chi'_R)$. The expression (8) is formally the same form as $S(Q,\omega)$ for phonons in solids[39,40] in which scattering from single phonons, pairs of phonons, and one-two phonon interference terms are retained.

The general result (8) has several interesting features[17] which motivated this experiment. Within this description of superfluid $^4$He, $S(Q,\omega)$ contains a singular part, proportional to $n_0$, which involves excitation of a single quasiparticle having wave vector $Q$. Thus any pole in the single quasiparticle Green's function $G_{\alpha\beta}(Q,\omega)$ will be observed in $S(Q,\omega)$ when $n_0\neq 0$. Since $n_0=N_0/N\lesssim 0.1$, the intensity in $S(Q,\omega)$ resulting from $\chi_S$ may be small. For $T>T_\lambda$, in the normal phase, the poles in $G_{\alpha\beta}$ can no longer be observed in $S(Q,\omega)$.

The $\chi'_R(Q,\omega)$ is the dynamic susceptibility involving quasiparticles above the condensate. As in liquid $^3$He and heavier fluids, $\chi'_R(Q,\omega)$ may display a collective (sound) mode, at least at low $Q$. It is this mode in $\chi'_R$ [strictly in the total $\chi(Q,\omega)$], which is discussed by Feynman[3] and evaluated in detail using correlated basis function methods.[4] Both $\chi_S$ and $\chi'_R$ can contain singular structure arising from long-lived quasiparticles and a collective density mode, respectively. Unfortunately, the spectral shape of $G_{\alpha\beta}$, $\Lambda(Q,\omega)$, and $\chi'_R(Q,\omega)$ is not known for strongly interacting fluids. When both $\chi'_R$ and $\chi_S$ have sharp, singular structure, it may not be useful to separate $\chi$ into two parts.

Gavoret and Nozières[7] show that the total $\chi(Q,\omega)$ and single-particle Green's functions in $G_1(Q,\omega)$ have a single common pole as $Q\to 0$. This occurs at frequency $\omega=cQ$ where $c$ is the macroscopic sound velocity. Thus as

$Q \rightarrow 0$ it is not meaningful to distinguish between single-particle and collective density excitations—there is only a single excitation at $\omega = cQ$, as shown by Bogolubov in the dilute gas limit. As $Q = 0.4$ Å$^{-1}$ the observed $S(Q,\omega)$ in Figs. 5 and 6 is concentrated almost entirely in a single peak with a very small tail reaching to higher $\omega$ This is true in both the superfluid and normal phases. This single peak is most readily interpreted[41] as due chiefly to a collective mode in $\chi'_R$ at $T < T_\lambda$ and a collective mode in the total $\chi$ for $T > T_\lambda$. For $T < T_\lambda$ the intensity due to $\chi_S$ must also lie in the same single peak. Indeed, if $Q = 0.4$ Å$^{-1}$ may be regarded as low $Q$, then we expect $G_1$ and $\chi$ to peak at the same energy.[7] The present resolution width $\Gamma_G \approx 1$ K is certainly not small enough to resolve two closely lying peaks, if $G_1$ and $\chi'_R$ peak at slightly different energies. Also, since $n_0 \lesssim 0.1$ most of the observed intensity in the single peak is probably due chiefly to $\chi'_R$ rather than $\chi_S$. On the basis of comparison with liquid $^3$He and other fluids, we expect $\chi$ to show rather little temperature dependence.

In contrast, at the maxon and roton $Q$ vectors, $S(Q,\omega)$ consists of a sharp peak superimposed on a broad background in the superfluid phase. Particularly at $Q = 1.13$ Å$^{-1}$, a large fraction of the intensity lies in the broad background (see Fig. 19). We might interpret the sharp peak as the single quasiparticle peak of $G$ in $\chi_S$ and the broad background as due to $\chi'_R$. In this case $\chi'_R$ does not contain a collective mode in the superfluid phase. As $T$ is increased, the sharp peak in $S(Q,\omega)$ decreases in intensity. This is expected from (8) since $\chi_S$ may continue to have sharp structure for $T > T_\lambda$, but the contribution to $\chi$, which is what is observed by neutrons, decreases with $n_0(T)$ and vanishes at $T_\lambda$. At $T > T_\lambda$ in the normal phase we observe only $\chi = \chi'_R$ which, from the discussion in Sec. VI B, does not appear to show a collective mode. This interpretation suggests that $\chi'_R$ is broad and does not have singular structure in both phases. In this case the separation of $\chi$ into $\chi_S$ and $\chi_R$ is very useful and offers a possible interpretation of the data not open to other formulations. This picture, originally suggested by Woods and Svensson,[20] is especially attractive at $Q = 1.13$ Å$^{-1}$. In the roton region the data are not so clear because the roton energy is low, and above $T_\lambda$ it is not clear whether $\chi$, has a collective mode or not. However, from Fig. 13 the sharp roton peak seen in the superfluid phase does seem to disappear at $T_\lambda$. Also, at the roton $Q$ we find $\Gamma(Q,T) > \omega(Q,T)$ for $T > T_\lambda$ when (2) is fitted to the observed intensity. This is uncharacteristic of a well-defined single mode suggesting the intensity is not due to scattering from a single mode. This also means that fitting (2), a single mode expression, to the observed intensity is not meaningful for $T > T_\lambda$ at the roton $Q$.

In this picture, the phonon and roton regions are significantly different. The $\chi$ contains a collective mode at low $Q$ but not for $Q \gtrsim 1.1$ Å$^{-1}$. At low $Q$ the peak in $S(Q,\omega)$ is predominantly due to the collective mode in $\chi$. As $Q \rightarrow 0$ it is meaningless to distinguish the peak in $\chi$ and $G$ since there is only one mode having a single energy. At $Q \gtrsim 1.1$ Å$^{-1}$ the sharp peak in $S(Q,\omega)$ for $T < T_\lambda$ is the quasiparticle peak in $G$. In this model liquid $^4$He does not support a collective density mode at higher $Q$. The sharp peak in $S(Q,\omega)$ disappears at $T_\lambda$ because $G$ no longer contributes to $S(Q,\omega)$ when $n_0(T) = 0$. Thus liquid $^4$He apparently behaves like a normal cold liquid in that it supports a collective density mode at small wave vector and this mode dominates $S(Q,\omega)$. In addition, the existence of a finite $n_0$ in the superfluid phase means that single quasiparticle excitations can be observed in $S(Q,\omega)$ and these constitute the sharp component of $S(Q,\omega)$ in the superfluid at larger wavevectors. This interpretation will be elaborated further in a forthcoming paper (Glyde and Griffin).

## ACKNOWLEDGMENTS

The authors wish to thank S. Hayden, D. Marcenac, D. Puschner, and C. C. Tang for assistance with the experiments and data treatment. Valuable discussions with Professor A. Griffin are gratefully acknowledged. They are grateful to the Institut Laue-Langevin for making available the experimental facilities used in this study and gratefully acknowledge the award of a North Atlantic Treaty Organization (NATO) collaboration grant. Support from the U.S. Department of Energy, Office of Basic Energy Sciences, under Contract No. DE-FG02-84ER45082 and from the Science and Engineering Research Council is also gratefully acknowledged.

[1]For reviews see, A. D. B. Woods and R. A. Cowley, Rep. Prog. Phys. **36**, 11 (1973); D. L. Price, in *The Physics of Liquid and Solid Helium,* edited by J. B. Ketterson and K. H. Bennemann (Wiley Interscience, New York, 1978), Vol. II, Chap. 19; H. R. Glyde and E. C. Svensson, in *Methods of Experimental Physics,* edited by K. Sköld and D. L. Price (Academic, New York, 1987), Vol. 23, Pt. C.

[2]L. D. Landau, J. Phys. (Moscow) **5**, 71 (1941); **11**, 91 (1947).

[3]R. P. Feynman, Phys. Rev. **91**, 1301 (1953); **94**, 262 (1954); R. P. Feynman and M. Cohen, *ibid.* **102**, 1189 (1956).

[4]C. W. Woo, in *The Physics of Liquid and Solid Helium* (Ref. 1), Vol. I, Chap. 5, p. 349; E. Manousakis and V. R. Pandharipande, Phys. Rev. B **33**, 150 (1986), and references therein.

[5]S. T. Beliaev, Zh. Eksp. Teor. Fiz. **34**, 417 (1958) [Sov. Phys.—JETP **7**, 289 (1958)].

[6]N. Hugenholtz and D. Pines, Phys. Rev. **116**, 489 (1959).

[7]J. Gavoret and P. Nozières, Ann. Phys. (N.Y.) **28**, 349 (1964).

[8]K. Huang and A. Klein, Ann. Phys. (N.Y.) **30**, 203 (1964).

[9]P. C. Hohenberg and P. C. Martin, Ann. Phys. (N.Y.) **34**, 291 (1965).

[10]V. Ambegoakar, J. M. Conway, and G. Baym, in *Lattice Dynamics,* edited by R. F. Wallis (Pergamon, New York, 1965), p. 261, Eq. (2.15).

[11]S. K. Ma and C. W. Woo, Phys. Rev. **159**, 165 (1967).

[12]S. K. Ma, H. Gould, and V. K. Wong, Phys. Rev. A **3**, 1453 (1971).

[13]I. Kondor and P. Szépfalusy, Acta Phys. Hung. **24**, 81 (1968); P. Szépfalusy and I. Kondor, Ann. Phys. (N.Y.) **82**, 1 (1974).

[14]H. Gould and V. K. Wong, Phys. Rev. Lett. **27**, 301 (1971).
[15]V. K. Wong and H. Gould, Ann. Phys. (N.Y.) **83**, 252 (1974).
[16]A. Griffin and T. H. Cheung, Phys. Rev. A **7**, 2086 (1973).
[17]A. Griffin, Can. J. Phys. **65**, 1368 (1987).
[18]K. Bedell, D. Pines, and A. Zawadowski, Phys. Rev. B **29**, 102 (1984).
[19]L. D. Landau and I. M. Khalatnikov, Zh. Eksp. Teor. Fiz. **19**, 637 (1949).
[20]A. D. B. Woods and E. C. Svensson, Phys. Rev. Lett. **41**, 974 (1978).
[21]E. C. Svensson, P. Martel, V. F. Sears, and A. D. B. Woods, Can. J. Phys. **54**, 2178 (1976).
[22]E. F. Talbot, H. R. Glyde, W. G. Stirling, and E. C. Svensson, Phys. Rev. B **38**, 11 229 (1988).
[23]A. D. B. Woods, Phys. Rev. Lett. **14**, 355 (1965).
[24]R. A. Cowley and A. D. B. Woods, Can. J. Phys. **49**, 177 (1971).
[25]F. Mezei and W. G. Stirling, in *75th Jubilee Conference on Helium-4,* edited by J. G. M. Armitage (World Scientific, Singapore, 1983), p. 111.
[26]A. Miller, D. Pines, and P. Nozières, Phys. Rev. **127**, 1452 (1962).
[27]F. Mezei, Phys. Rev. Lett. **44**, 1601 (1980).
[28]J. A. Tarvin and L. Passell, Phys. Rev. B **19**, 1458 (1979); K. S. Pedersen and K. Carneiro, *ibid.* **22**, 191 (1980).
[29]R. Scherm, K. Guckelsberger, B. Fäk, K. Sköld, A. J. Dianoux, H. Godfrin, and W. G. Stirling, Phys. Rev. Lett. **59**, 217 (1987).
[30]D. Hess and D. Pines, J. Low Temp. Phys. **72**, 247 (1988).
[31]H. R. Glyde and F. C. Khanna, Can. J. Phys. **58**, 343 (1980).
[32]H. G. Bell, A. Kollmar, B. Allfeld, and T. Springer, Phys. Lett. **45A**, 479 (1973).
[33]W. J. L. Buyers, V. F. Sears, P. A. Lonngi, and D. A. Lonngi, Phys. Rev. B **11**, 697 (1975).
[34]J. R. D. Copley and J. M. Rowe, Phys. Rev. Lett. **32**, 49 (1974); A. Rahman, *ibid.* **32**, 52 (1974).
[35]G. Jacucci, in *Condensed Matter Research Using Neutrons,* edited by S. W. Lovesey and R. Scherm (Plenum, New York, 1984).
[36]K. Sköld and C. A. Pelizzari, Philos. Trans. R. Soc. London, Ser. B **290**, 605 (1980).
[37]N. N. Bogolubov, J. Phys. (Moscow) **11**, 23 (1947).
[38]E. C. Svensson, P. Martel, V. F. Sears, and A. D. B. Woods, Can. J. Phys. **54**, 2178 (1976).
[39]R. A. Cowley and W. J. L. Buyers, J. Phys. C **2**, 2262 (1969).
[40]H. R. Glyde, Can. J. Phys. **52**, 2281 (1974).
[41]D. Pines, in *Quantum Fluids,* edited by D. F. Brewer (North-Holland, Amsterdam, 1966), p. 257.